Determination of Semi-Transparent Cirrus Cloud Temperature from Infrared Radiances: Application to METEOSAT

GERARD SZEJWACH[1]

Laboratoire de Meteorologie Dynamique, CNRS, École Polytechnique, Palaiseau, France

(Manuscript received 20 May 1981, in final form 29 November 1981)

ABSTRACT

The use of simultaneous infrared measurements to derive the temperature and emissivity of semi-transparent cirrus clouds is experimentally investigated. Results from the NASA/CONVAIR-990 Winter Experiment Program, 1977 (WEP) are discussed. It is shown that the mean effective emissivities of cirrus in the water vapor absorption channel 5.7–7.1 μm and in the window channel 10.5–12.5 μm are equal to within 6%. A method is then developed to derive the cirrus temperature and emissivity from simultaneous measurements in the two infrared channels. This method is applied to 14 cirrus cloud cases observed during the WEP experiment. The infrared temperature was found to agree with other aircraft or conventional data. A similar technique is then developed and applied to METEOSAT digital images. The results indicate that using both infrared channels should lead to a major improvement in the determination of the cirrus cloud temperature and height from satellites.

1. Introduction

Cirrus clouds are very often semi-transparent in the infrared part of the electromagnetic spectrum. It is therefore not possible to determine both their emissivity and their temperature (two unknowns) from measurements made in a single channel. Bi-spectral methods have been developed to determine these parameters from satellite measurements. These techniques involve an infrared window channel (around 11 μm) and a visible channel as shown by Shenk and Curran (1973), Park *et al.* (1974), Vonder Haar and Reynolds (1974) and Reynolds and Vonder Haar (1977). These methods, which are very sensitive to the relationship between the visible reflectivity and the infrared emissivity of the cloud have the major deficiency of not being useful at night. The purpose of this paper is to pursue a bi-spectral method to infer the cirrus cloud-top temperature, which uses two infrared channels; one in the water vapor absorption region around 6.5 μm and the other one centered at 11.5 μm in the Simpson window. The relationship between the cloud emissivity in both channels has been theoretically and experimentally investigated. In order to test the theory an experiment has been conducted during March and April of 1977 in the vicinity of the west coast of the United States. During this experiment simultaneous measurements in the two infrared channels of the high resolution LMD/ARIES radiometer were obtained over cirrus clouds associated with extratropical disturbances.

The results, concerning the mean effective emissivity in both channels, led to the development of the technique for the determination of the cloud parameters. This technique is applied to the observed cirrus, and then derived temperatures are compared to *in-situ* measurements.

The results obtained from the aircraft experiment show that the cirrus temperature inferred from our technique is closer to the thermodynamic cirrus temperature than the brightness temperature measured in either the window (11.5 μm) or the water vapor absorption (6.5 μm) channel.

A similar method is then applied to several cirrus cloud cases observed on METEOSAT.

Although no good calibration data were available for the date of observation, quantitative and qualitative results indicate that our method should lead to an improvement in the determination of semi-transparent cirrus temperatures as compared to those inferred from one infrared channel only.

2. Instrumentation and calibration

The high resolution ARIES radiometer (Fig. 1) was designed and constructed at Laboratoire de Meteorologie Dynamique, CNRS, France. It is a multichannel scanning radiometer with two digital (8-bits) and two analog channels. For the purpose of this experiment the two digital channels were chosen as follows: Channel 1: from 5.7 to 7.1 μm in a region of water vapor absorption, and Channel 2:

[1] Present affiliation: NASA/GLAS/Code 915, Goddard Space Flight Center, Greenbelt, MD.

0021-8952/82/030384-10$06.50

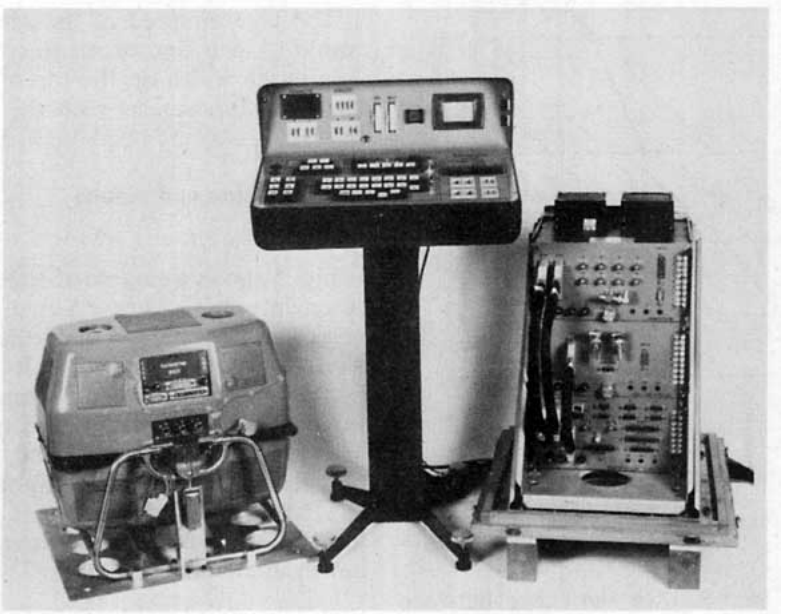

FIG. 1. ARIES radiometer.

from 10.5 to 12.5 μm in the Simpson window (Fig. 2). General performance characteristics of the radiometer are given here and a more complete and detailed description is given by Szejwach (1980).

The instantaneous field of view is 2.8×10^{-3} rad. Each line is comprised of 900 points with an overlap of ⅓ between two adjacent points. The total scanning angle is equal to 90°. The sampling between the lines is given by the speed of the aircraft and the speed of rotation of the radiometer's dichroic mirror which can be set equal to 4.55, 9.1, 18.2 or 36.4 rotations per second.

The inflight calibration is ensured by two internal automatically regulated blackbodies whose temperatures can be set between 250 and 335 K. A laboratory calibration of the instrument has been performed before and after the experiment in addition to the inflight calibration.

The Noise Equivalent temperature uncertainty NEΔT of the instrument for flight conditions has been found equal to 0.18 K for the window channel with a scene temperature equal to 280 K and to 1.15 K for the water vapor channel and a field of view temperature of 240 K; this larger error is due to the poor response of the detector in this spectral region and also to the fact that for the same blackbody temperature the signal received by the detector is considerably smaller in the water-vapor channel than in the window channel.

During the Winter Experiment Program conducted by NASA in 1977, the ARIES radiometer was mounted on board the AMES/CONVAIR-990 for 16 experimental flights. The Airborne Digital Data Acquisition System (ADDAS) provided meteorological parameters as well as navigation data.

Conventional radiosondes taken at San Diego were also used for comparison with our data. Meteosat data from the visible, window and water vapor channels were analyzed and processed on the LMD interactive facility, DIVISET.

3. Cloud observation and measurements

Measurements and results discussed in this paper concern cirrus clouds observed during flight 10 of the NASA/CONVAIR-990 Winter Experiment Program on March 25, 1977. Fourteen different cirrus clouds were studied between 2000 and 2400 GMT in the vicinity of San Diego.

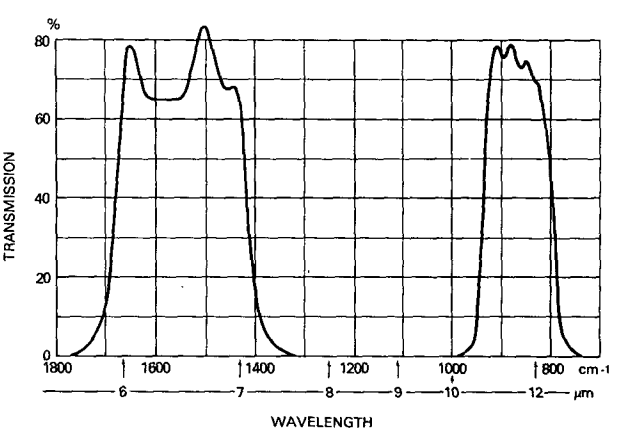

FIG. 2. Transmission function of ARIES filters.

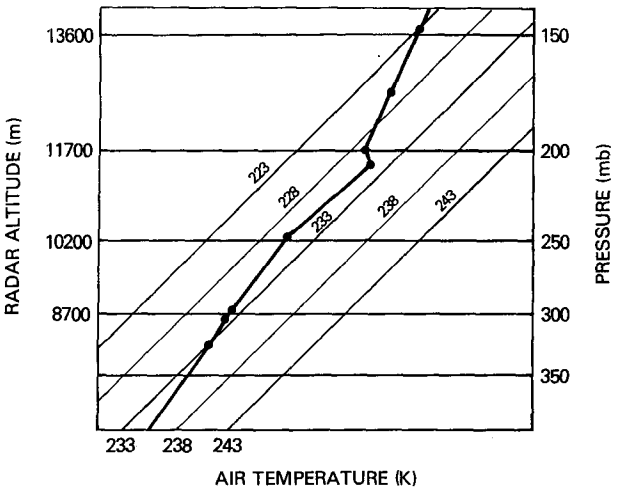

FIG. 3. San Diego sounding: 26 March 1977 at 0000 GMT.

The clouds were located over the ocean between 9000 and 10 000 m above sea level. The maximum flight level was 12 500 m. Both the 0000 GMT sounding (Fig. 3) and aircraft data indicated that the air temperature between 8900 and 11500 m was constant within 1 K (231 K). It is assumed that the clouds were in thermodynamic equilibrium with the surrounding atmosphere, and that they were isothermal. The flight pattern is given on Fig. 4. The CONVAIR-990 flew one horizontal straight-and-level leg at the maximum flight level (12 500 m), then a second leg at ~100 m above the cloud upper surface and a third leg at the cloud base level (~9000 m) in order to measure the incoming radiation at the cloud base. The horizontal extent of the legs varied from 3 to 20 km depending on the size of the cirrus cloud.

The true airspeed of the aircraft was 230 m s^{-1} resulting in a line of measurements every 50.5 m. The swath width on the top of the cloud depended on the difference between the flight and cloud-top levels.

4. Discussion and results

a. Nadir brightness temperatures

Fig. 5 shows a sample of simultaneous nadir measurements obtained over a cirrus cloud in both channels. The *X*-axis represents the horizontal distance along the path of the aircraft, the *Y*-axis indicates the equivalent blackbody temperature of the measured radiances in the water vapor absorption channel (1) (right hand side) and the window channel (2) (left hand side). The flight level here is 12500 m. The following features can be observed on Fig. 5 and Fig. 6 which represent two digital images obtained in channels 1 and 2.

i) The nadir brightness temperature observed over the ocean outside the cloud is ~40 K colder in the water-vapor channel 1 than in the window channel 2.

ii) The nadir-brightness temperature of the cloud upper surface is always warmer than the cloud thermodynamic temperature: 231 K ± 1 K. Therefore a single measurement in either channel will not determine the cloud temperature.

iii) Over the cirrus cloud the brightness temperatures are systematically colder in the absorption channel 1 than in the window channel 2.

iv) There is a very good spatial correlation over the cloud surface of both brightness temperatures.

Let us first consider the radiation observed over the ocean in absence of clouds. We measured the

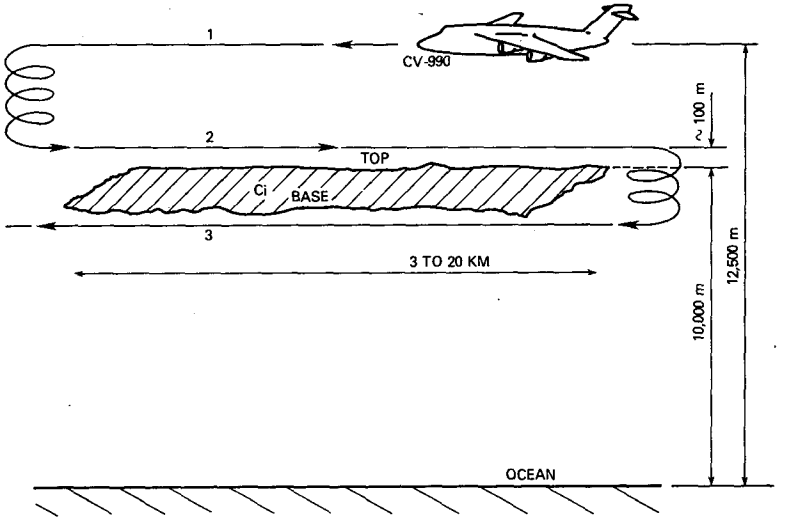

FIG. 4. CONVAIR-990 Flight pattern.

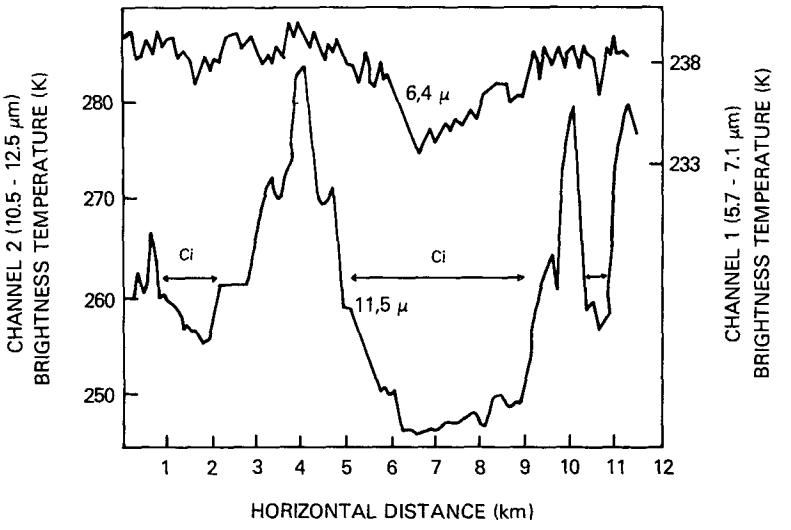

FIG. 5. Sample simultaneous nadir measurements over a cirrus cloud from the water vapor and window channels. Flight level 12 500 m.

nadir brightness temperature over the ocean at three different flight levels: at 12 500 m above the surface, at the cloud-top level around 10 000 m and at the cloud-base level near 9000 m. At the flight level of 12 500 m as seen on Fig. 5, we observed a value of 241.5 ± 0.75 K in the 6.5 μm water vapor channel and 283.4 ± 0.3 K in the 11.5 μm window channel. Similar values within the accuracy of the measurement were observed at 10 000 m. At the cloud-base level, the nadir brightness temperature over the ocean in absence of clouds was found equal to 243.0 K ± 0.75 K in the water vapor channel while the window channel temperature remained unchanged.

Hence, the upward radiation reaching the cloud base appears 40 K colder in the water vapor channel than in the window channel. This is due to the fact that in the window channel, the radiation emitted by the sea surface is only slightly modified by the atmosphere, while in Channel 1 this radiation is completely absorbed by the water vapor present between the ocean and the cloud base and reemitted at lower-atmospheric temperatures. The brightness temperature of the radiation received by the instrument in the water-vapor channel depends upon both temperature and humidity vertical profiles between the sensor and the ground and on the spectral response of the instrument in that channel. In our case the radiation in the water vapor channel corresponds to the air temperature at 480 mb (5650 m) when the sensor is located at 12 500 m. At the cloud-base level, the brightness temperature of the clear atmosphere in channel 1 is 1.5 K warmer; this means that the water vapor present between the cloud base level near 9000 and 12 500 m is still absorbing the upward radiation; but the fact that no noticeable brightness temperature difference appeared in this channel when measurements were performed at 12 500 m and at the cloud-top levels indicate that the effects of absorption by the water vapor above the cloud upper surface was negligible.

Let us now consider the radiation emerging from the cirrus upper surface. This amount of radiation is the sum of the radiation reaching the cloud base, transmitted after absorption and scattering by ice crystals and water vapor present inside the cloud, and the radiation emitted by the absorbing particles at their thermodynamic temperature. If the cloud was a blackbody with an emissivity equal to unity, we would observe in both channels the same brightness temperature: 231 K ± 1 K, the cloud thermodynamic temperature, since as noted above there is no noticeable absorption by water vapor above the cloud top. The brightness temperature measured over the cirrus in both channels was found always warmer than the cloud thermodynamic temperature. This indicates that the cirrus observed were semi-transparent. If the cloud were totally transparent we would observe in each channel the same brightness temperature as the one measured at the cloud-base level, 243 and 283.4 K in the water vapor and window channels, respectively. Any value of the emissivity between 1 and 0 will yield to a brightness temperature ranging from 231 to 243 K in channel 1 and 231 to 283.4 K in channel 2.

The fact that the brightness temperatures over the cirrus are systematically colder in the absorption channel than in the window channel can be attributed either to a larger value of the cloud emissivity in channel 1 than in channel 2 or to the "colder" radiation reaching the cloud base in the first channel.

There is a good spatial correlation over the cloud surface of both 6.5 and 11.5 μm brightness temper-

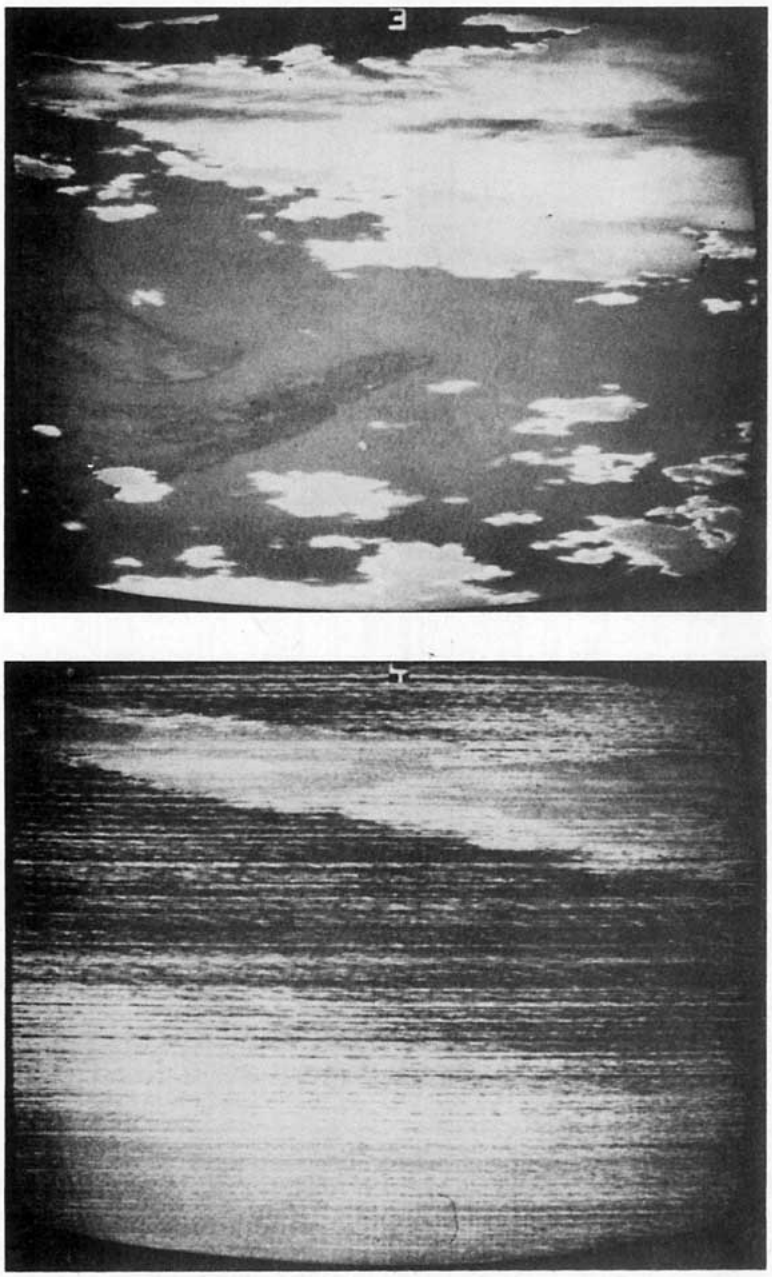

FIG. 6. Sample of simultaneous measurements over a cirrus cloud from ARIES digital image. Top: window channel: 10.5–12.5 μm. Bottom: water vapor channel: 5.7–7.1 μm.

atures. This suggests the existence of a relationship between the cloud effective emissivities in both channels when traveling over areas of different optical thickness, assuming that the cloud is isothermal.

The relationship between brightness temperatures (T_{BB}) observed simultaneously over the same cloud patterns is given in Fig. 7 where the water vapor channel brightness temperature is expressed versus the window channel brightness temperature. Colder temperatures correspond to optically thicker cloud regions. We note that if we extrapolate the curve to the left, the regression curve intersects the point corresponding to T_{BB} = 231 K in both channels, which is the brightness temperature of the cirrus if it were a black cloud. On the right-hand side, both T_{BB} values tend to the clear-air brightness temperatures as the cirrus becomes optically thinner and more transparent.

b. Effective emissivity in both channels

According to Paltridge and Platt (1976) a simplified radiation transfer equation where scattering is neglected and only the effects of absorption are considered can be written for each channel as follows:

Channel 1:

$$R_1 = \int_{5.7}^{7.1} \phi_\lambda B_\lambda(T_1)d\lambda = E_1 \int_{5.7}^{7.1} \phi_\lambda B_\lambda(T_N)d\lambda + (1 - E_1) \int_{5.7}^{7.1} \phi_\lambda B_\lambda(T_F)d\lambda, \quad (1)$$

Channel 2:

$$R_2 = \int_{10.5}^{12.5} \phi_\lambda B_\lambda(T_2)d\lambda = E_2 \int_{10.5}^{12.5} \phi_\lambda B_\lambda(T_N)d\lambda + (1 - E_2) \int_{10.5}^{12.5} \phi_\lambda B_\lambda(T_G)d\lambda, \quad (2)$$

where R_1 and R_2 are the radiances received in channels 1 and 2, respectively, T_1 and T_2 are the brightness temperatures, $B_\lambda(T)$ is the Planck function, ϕ_λ the spectral response of the instrument, e_λ the spectral emissivity, T_N the cloud temperature, T_F and T_G the brightness temperature of the incoming upward radiation at the cloud base level in channels 1 and 2, respectively, and the mean effective emissivity E_1 and E_2 for each channel is defined by

Channel i:

$$E_i = \int_{\lambda_1}^{\lambda_2} \phi_\lambda e_\lambda B_\lambda(T)d\lambda \int_{\lambda_1}^{\lambda_2} \phi_\lambda B_\lambda(T)d\lambda. \quad (3)$$

E_1 and E_2 can be derived from (1) and (2) and the measured values of R_1, R_2 (or T_1, T_2), T_F, T_G and T_N. The dots on Fig. 8 represent the values obtained from (1) and (2) and the measurements, for E_1 versus E_2 over simultaneously observed cirrus areas of various optical thickness. The dashed straight line is the 45° line. The curve on Fig. 8 is derived from theory as follows: We consider only the process of absorption-emission by spherical ice particles of radius r. The spectral emissivity e_λ is related to the volume absorption coefficient $Q_{a,\lambda}$ by

$$e_\lambda = 1 - \exp(-\pi \Delta Z Q_{a,\lambda} \int_0^\infty N(r)r^2dr), \quad (4)$$

where $N(r)$ is the number of ice particles per unit of volume of radius r, and ΔZ the cloud geometrical thickness. We used the values of $Q_{a,\lambda}$ for ice spheres of radius $r = 10$ μm from Irvine and Pollack (1968) to compute the mean volume absorption coefficient $Q_{a,i}$ in each channel. According to these authors $Q_{a,\lambda}$ does not change significantly when r becomes larger than 10 μm. The mean emissivity for each channel E_i is related to the mean volume absorption coefficient $Q_{a,i}$ by an equation similar to (4). E_1 is then simply related to E_2 by

$$(1 - E_1)^{Q_{a,2}} = (1 - E_2)^{Q_{a,1}}. \quad (4a)$$

The curve on Fig. 8 corresponds to values of $Q_{a,1}$ and $Q_{a,2}$ equal to 0.977 and 1.092, respectively. The dots obtained from the experiment are located in the vicinity of the theoretical curve but the most significant result is the fact that within 6% at most, the mean effective emissivity, as defined by (1) or (2) and (3), is the same in both water vapor and window channels.

Therefore, the differences between observed brightness temperatures in channels 1 and 2 over a semi-transparent cirrus cloud are due to the fact that the upward radiation reaching the cloud base is much "colder" in the water absorption channel 1 than in the window channel 2, and not to the fact that the cloud itself is more opaque in channel 1 than in channel 2.

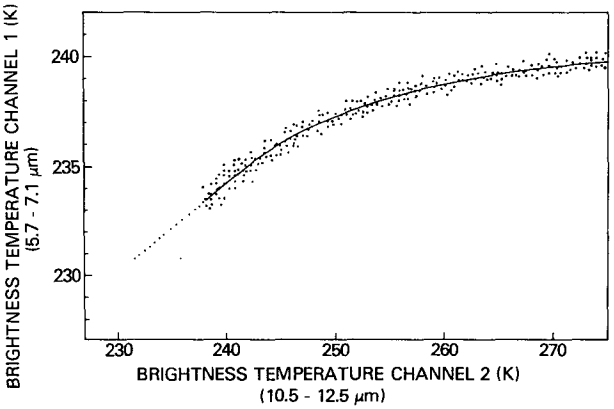

FIG. 7. Brightness temperature over a cirrus cloud, water-vapor channel (1) versus window channel (2).

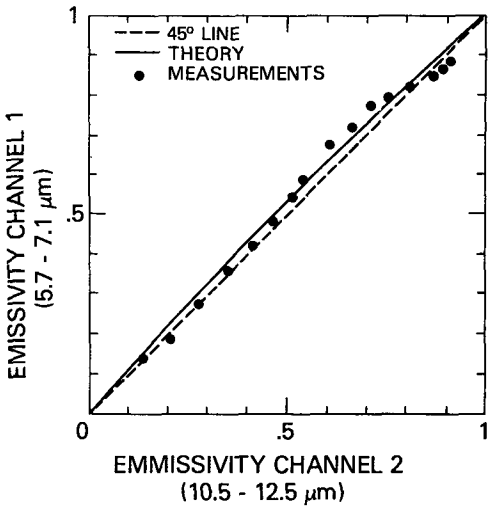

FIG. 8. Cirrus emissivity in the water-vapor channel (1) versus emissivity in the window channel (2).

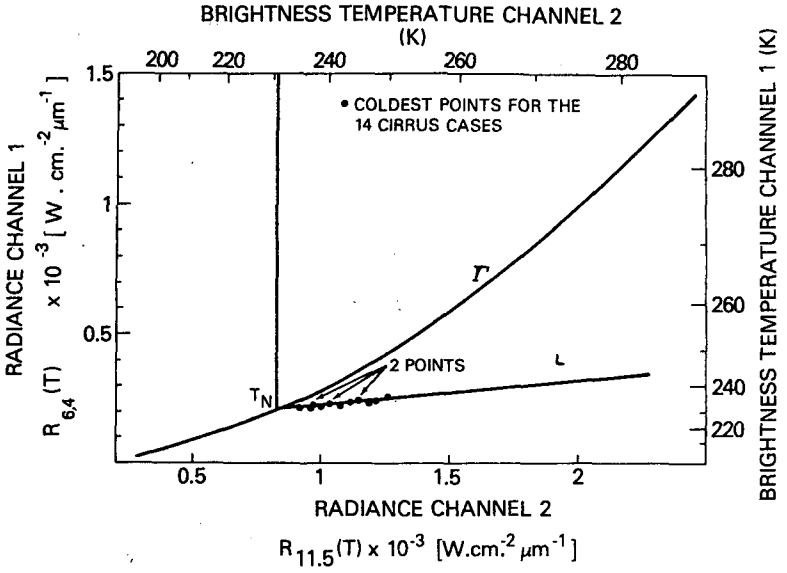

FIG. 9. Brightness temperatures and radiances of the optically thickest points of the 14 studied cirrus cases. Water-vapor channel (1) versus window channel (2).

c. Determination of semi-transparent cirrus temperature and emissivity

When absorption by water vapor above the cloud top is negligible, Eqs. (1) and (2) may be written as follows

$$R_1(T_1) = E_1 R_1(T_N) + (1 - E_1) R_1(T_F), \quad (5)$$

$$R_2(T_2) = E_2 R_2(T_N) + (1 - E_2) R_2(T_G). \quad (6)$$

We have seen above that the mean emissivity was the same in both channels. By elimination of E_i in (5) and (6) we obtain

$$R_1(T_1) = aR_2(T_2) + b, \quad (7)$$

where

$$a = [R_1(T_N) - R_1(T_F)]/[R_2(T_N) - R_2(T_G)]$$

and

$$b = [R_1(T_F)R_2(T_N) - R_1(T_N)R_2(T_G)]/[R_2(T_N) - R_2(T_G)].$$

Eq. (7) indicates that there is a linear relationship between R_1 and R_2 independent of the value of the cloud emissivity.

Hence, if we have a set of n measurements obtained in both channels over several areas of different optical thickness from the same cirrus clouds, the points $R_{2,j}(T_2)$, $R_{1,j}(T_1)$ with $j = 1$ to n belong to the same line L on a graph where $R_1(T)$ is expressed versus $R_2(T)$ as in Fig. 9.

On this graph, the curve Γ: $R_1(T) = fR_2(T)$ describes the radiation emitted simultaneously in both channels by blackbodies at a temperature T ranging from 200 to 288 K.

Therefore the intersection between L and Γ represents the emission temperature of a blackbody having the same temperature as the semi-transparent cirrus cloud that has been considered here.

It is important to note that the method is still valid when the field of view of the instrument is not completely covered by the cloud. In this case E should be replaced by the product NE (where N represents the fraction of cloud cover) in (5) and (6). By elimination of NE in those two equations we obtain the same Eq. (7).

Once T_N is determined, NE may be computed either from (5) or (6). Only the product NE is attainable with this technique.

Application of this method is given in Fig. 9 where the coldest simultaneous measured radiances are represented for the 14 observed cirrus clouds during flight 10. Since all the clouds have the same temperature, the representative points are aligned. The intersection between Γ and the line L gives the effective cloud temperature 231 K which agrees with other observations; and the line intersects the point R_2(283.4 K), R_1(243 K) as expected.

5. Application to METEOSAT data

The major differences between the aircraft data and METEOSAT digital images as far as this technique is concerned are the following:

1) The field of view of each pixel is considerably larger for METEOSAT and the probability for the fraction of cloud cover N to be equal to one is therefore much smaller in a satellite pixel; but this does not affect the validity of the method as demonstrated above.

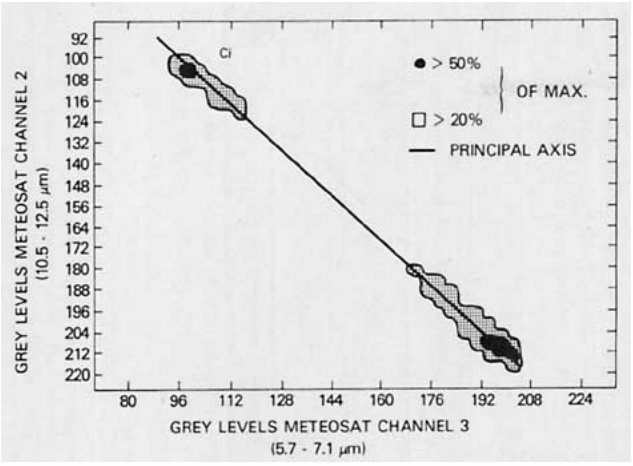

FIG. 10. Sample of bi-dimensional histogram obtained over a cirrus cloud on METEOSAT digital images water vapor channel (3) and window channel (2).

2) In our case absorption by water vapor above the cloud top was negligible; this is generally not true except for very high cirrus, and it is difficult to take this effect into account without other observations like a sounding or a model. For most cases on METEOSAT images the absorption by water vapor above the cloud top should be taken into account.

3) The incoming radiation at the cloud base is not defined by satellite observation: this parameter does not need to be defined for the cloud temperature determination but this is not true for the computation of the product *NE*.

4) The calibration of the water-vapor channel for the METEOSAT data considered in this study was not accurate enough for the purpose of comparison with other data (aircraft or sounding).

The method to determine the cloud temperature was modified as follows: We have seen that two measurements of data points are sufficient to determine the cloud temperature from the intersection of Γ and L. We take a slightly different approach for METEOSAT data. We consider image segments of 64 lines by 64 points around the observed cirrus.

Each point of the image segment is characterized by a couple (R_2, R_3) where R_2 and R_3 are the grey levels proportional to the radiances observed in the window channel 2 and water vapor channel 3 of METEOSAT. We perform a bi-dimensional histogram of these grey levels: we compute the frequency of occurrence of points having a given couple (R_2, R_3) of grey levels in channel 2 (Y-axis) and channel 3 (X-axis). Fig. 10 gives an example of such bi-dimensional histogram. We note F_{MAX}, the largest frequency observed. The dots represent areas with frequencies of occurrence larger than 0.2 F_{MAX} and the black regions correspond to occurrences larger than 0.5 F_{MAX}.

We determine the principal axis of the histogram using a least-square fitting for all couples (R_2, R_3) corresponding to the cirrus. This defines the line L; Γ is defined from the calibration curves. The intersection between Γ and L gives the value of the cloud temperature T_N. Table 1 gives the results for 5 cases corresponding to Fig. 11a, b, on 23 July 1978. The calibration curve for channel 3 was questionable for this time period; therefore the quantitative result may not be compared to other information. However,

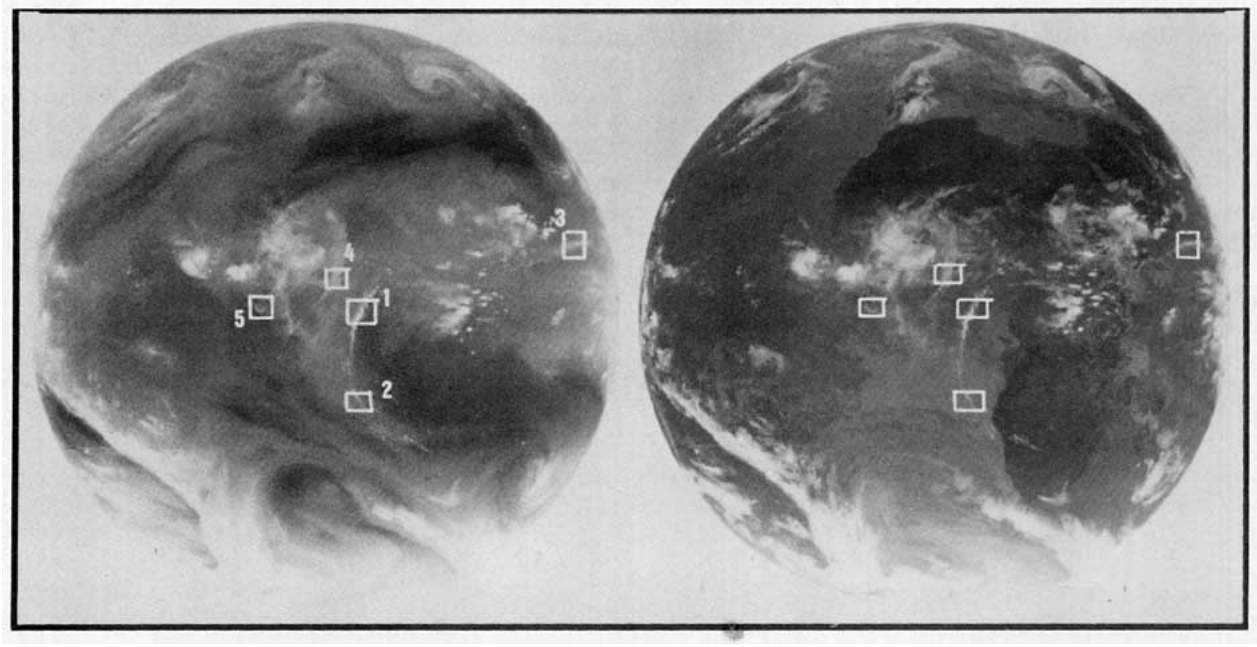

FIG. 11. METEOSAT images from 23 July 1978; 1200 GMT. Left: Window channel. Right: Water-vapor channel.

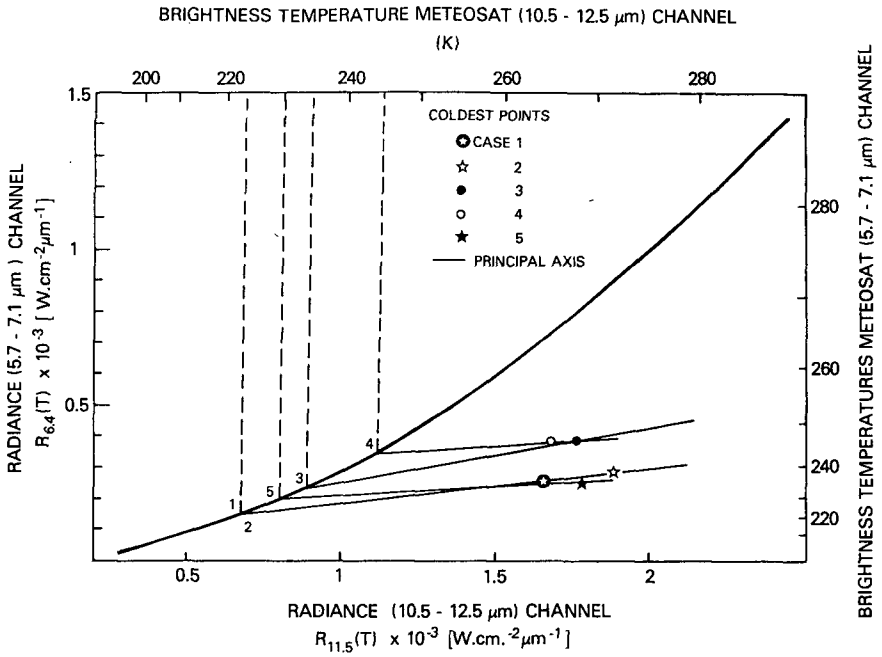

FIG. 12. Principal axis, coldest points and inferred cirrus temperature observed for the five METEOSAT cases.

the inferences from the observed results should remain valid with a more appropriate calibration. Fig. 12 presents the five regression lines (or principal axis), obtained as described above, of the bi-dimensional histogram for the five cases. Also indicated on the figure are the coldest points observed for each case and the intersection with Γ which gives the inferred cloud temperature T_N.

The following conclusions can be made from the results displayed in Table 1.

1) The brightness temperature is always much warmer in the window channel than in the water-vapor channel, as expected. As discussed above this is not because cirrus clouds are more transparent in the window channel (2) than in the water-vapor channel (3) but mainly because the incoming radiation at the cloud base is "colder" in the water-vapor channel than in the infrared channel and also for some cases (relatively low cirrus) because of the presence of a nonnegligible amount of water vapor above the cloud top (these two effects leading to a colder T_{BB}).

2) Cases 1 and 2 yield to the same cloud temperature. If we look at Fig. 11, cases 1 and 2 are related to the same cirrus band; the further south the band extends the thinner the cloud appears. This is confirmed by both window and water-vapor channel brightness temperatures. However, the cloud level should be the same for both cases and the inferred cloud temperature from the method described in this paper confirms this fact.

3) The coldest points of cases 3 and 4 are very close to each other, indicating a comparable cloud temperature. The temperatures inferred from our method shows a difference of ~13 K between both cloud temperatures; unfortunately no other type of observation was available to confirm this result.

TABLE 1. Brightness temperatures for channel 2 and 3 of five METEOSAT cases and inferred cloud temperature from our method.

Case	Latitude central point	Longitude central point	Coldest point: T_{BB} (K) Window channel 2	Coldest point: T_{BB} (K) Water vapor channel 3	Cloud temperature from our method, T_N (K)
1	0.13 N	5.35 E	263.5	236.2	222.5
2	12.97 S	5.55 E	274.3	239.3	222.5
3	13.41 N	55.93 E	268	247.2	231.0
4	7.34 N	2.14 E	265.7	246.6	244.0
5	1.18 N	−10.54 W	268	236.2	226.0

6. Conclusion and future work

Simultaneous infrared airborne measurements were performed over semi-transparent cirrus clouds in the following channels: Channel 1 (5.7–7.1 μm) and channel 2 (10.5–12.5 μm). Data analysis indicates that within 6% the cloud effective emissivity is the same in both channels. This result led to the development of a bispectral method to infer the temperature of such clouds. Application of this technique to aircraft data and comparison with conventional and airborne measurements confirm the validity of the method. A slightly modified version of the technique is used for application to the geosynchroneous satellite METEOSAT. This method may also be applied by using the two equivalent channels of the GOES 4 VISSR Atmospheric Sounder (VAS). In the case of METEOSAT, cirrus temperatures derived from our method appeared to be much colder than the observed blackbody temperatures in both channels. Qualitative and quantitative considerations indicate that the application of our method should lead to a major improvement in the determination of the temperature and height of semi-transparent cirrus clouds. The effects of absorption by water vapor which might be present above the cloud top have not been taken into account here. Corrections could be applied if the temperature and humidity profiles in the vicinity of the clouds are known.

Aircraft measurements were performed during the SESAME 79 (Severe Environmental Storm and Mesoscale Experiment) over cirrus clouds associated with severe local storms. In SESAME, as indicated by the preliminary results, there was non-negligible water vapor above the cirrus cloud top. Analyses in which we take into account the absorption by this water vapor are now in progress.

Acknowledgments. I would like to thank J. L. Monge, F. Sirou and A. Gilet who designed ARIES, installed the instrument on board the NASA/CONVAIR-990 and participated in the experiment. This study was made possible thanks to the help of W. Shenk, Dr. A. F. Hasler and the Goddard Laboratory for Atmospheric Sciences, NASA who supported our flights. E. Peterson from Ames Research Center, NASA planned and managed our flight program. I also wish to thank Dr. H. J. Cooper for useful discussions and Esther Gray for her fast and accurate typing.

REFERENCES

Irvine, W. M., and G. B. Pollack, 1968: Infrared optical properties of water and ice spheres. *Icarus*, **8**, 324–360.

Paltridge, G. W., and C. M. R. Platt, 1976: *Radiative Processes in Meteorology and Climatology*. Elsevier, 318 pp.

Park, S. U., D. N. Sikdar and V. E. Suomi, 1974: Correlation between cloud thickness and brightness using Nimbus-4 THIR data and ATS-3 digital data. *J. Appl. Meteor.*, **13**, 402–410.

Reynolds, D. W., and T. H. Vonder Haar, 1977: A bi-spectral method for cloud parameter determination. *Mon. Wea. Rev.*, **105**, 446–457.

Shenk, W. E., and R. J. Curran, 1973: A multispectral method for estimation of cirrus cloud top heights. *J. Appl. Meteor.*, **12**, 1213–1216.

Szejwach, G., 1980: Contribution ā l'étude du rayonnement infrarouge des nuages. Application à la reconstitution tridimensionnelle de la couverture nuageuse. Thèse de Doctorat d'Etat, Université P. et M. Curie (Paris), 210 pp.

Vonder Haar, T. H., and D. W. Reynolds, 1974: A bi-spectral method for inferring cloud amount and cloud-top temperature using satellite data. *Preprints 6th Conf. Aerospace and Aeronautical Meteorology.*, El Paso, Amer. Meteor. Soc.